Time-Dependent Phase Segregation of Dendrimer/*n*-Alkylthiol Mixed-Monolayers on Au(111): An Atomic Force Microscopy Study

William M. Lackowski, Joseph K. Campbell, Grant Edwards, Victor Chechik, and Richard M. Crooks*

Department of Chemistry, P.O. Box 30012, Texas A&M University, College Station, Texas 77842-3012

Received March 26, 1999. In Final Form: June 2, 1999

The two-dimensional phase behavior of mixed-monolayers composed of poly(amidoamine) (PAMAM) dendrimers and *n*-alkylthiols adsorbed to Au(111) surfaces was studied using tapping mode atomic force microscopy (TM-AFM). Mixed-monolayers were prepared by sequential immersion of Au(111) substrates into ethanolic solutions of, first, dendrimers and then *n*-alkylthiols. Films were prepared by systematically varying the dendrimer generation (G4, G6, and G8) and the *n*-alkylthiol chain length ($CH_3(CH_2)_xSH$; $x = 4, 11, 15$). TM-AFM was used to monitor time-dependent morphological changes in the mixed-monolayers. Dendrimer monolayers immersed in hexane solutions of *n*-alkylthiols do not phase separate to an appreciable extent, which demonstrates the important role of dendrimer solvation in these processes. In contrast to the amine-terminated dendrimer monolayers, thiol-terminated dendrimers do not phase separate when exposed to ethanolic *n*-alkylthiol solutions, suggesting that one of the driving forces for this process is the difference in adsorption energies between the amine and thiol groups and the Au substrate.

Introduction

Previously we showed that exposure of a Au(111)-adsorbed monolayer of poly(amidoamine) (PAMAM) dendrimers to an ethanolic solution of *n*-hexadecylthiol (C16SH) leads to a mixed PAMAM/C16SH monolayer in which the dendrimers are geometrically distorted. We also demonstrated that the dendrimers eventually desorb from the Au(111) surface and are completely replaced by C16SH.[1] Here, we expand upon this finding by studying the effect on monolayer morphology induced by varying the dendrimer generation and terminal group composition, *n*-alkylthiol chain length, and exposure time of the dendrimer monolayer to the *n*-alkylthiol solutions.

Interest in self-assembled thin films stems from their ease of preparation and potential use in such fields as chemical sensors,[2−4] lithography,[5−7] adhesion,[8−11] and corrosion inhibition.[12,13] We have previously shown that dendrimers spontaneously form nearly close-packed, monolayer-thick films when exposed to Au surfaces.[1,14] Dendrimers are roughly spherical polymers prepared by iterative attachment of branching monomers to a central core. Accordingly, the number of terminal groups on PAMAM dendrimers increases geometrically as a function of generation; that is, the second-generation PAMAM dendrimer (G2) has 16 terminal groups while G4 has 64. Among their many suggested applications, these fascinating materials have been studied as components of both supramolecular assemblies and organic thin films.[15−19] For example, we have shown that the properties of mixed-monolayers of dendrimers and *n*-alkylthiols exhibit characteristics of both constituents.[14] Incorporation of dendrimers into *n*-alkylthiol self-assembled monolayers (SAMs) increases the overall surface area of the monolayer and may increase the number of active terminal groups per unit area,[20] which is useful for chemical sensing applications.[18] Such mixed-monolayers also behave as simple models of ion-transport membrane proteins.[21]

Morphological changes in the composite monolayers were evaluated using tapping-mode atomic force microscopy (TM-AFM). The use of AFM to elucidate topographical information about surfaces on the submicron scale has been recently reviewed.[22,23] *n*-Alkylthiol monolayers,[23,24]

* To whom correspondence should be addressed. Tel: 409-845-5629; Fax: 409-845-1399; E-mail: crooks@tamu.edu.

(1) Hierlemann, A.; Campbell, J. K.; Baker, L. A.; Crooks, R. M.; Ricco, A. J. *J. Am. Chem. Soc.* **1998**, *120*, 5323−5324.
(2) Thomas, R. C.; Yang, H. C.; DiRubio, C. R.; Ricco, A. J.; Crooks, R. M. *Langmuir* **1996**, *12*, 2239−2246.
(3) Ricco, A. J.; Crooks, R. M.; Osbourn, G. C. *Acc. Chem. Res.* **1998**, *31*, 298−296.
(4) Crooks, R. M.; Ricco, A. J. *Acc. Chem. Res.* **1998**, *31*, 219−227.
(5) Xia, Y.; Whitesides, G. M. *Langmuir* **1997**, *13*, 2059−2067.
(6) Xia, Y.; Tien, J.; Qin, D.; Whitesides, G. M. *Langmuir* **1996**, *12*, 4033−4038.
(7) Corbitt, T. S.; Crooks, R. M.; Hampden-Smith, M. J.; Ross, C. B.; Schoer, J. K. *Adv. Mater.* **1993**, *5*, 930−931.
(8) Yamada, S.; Israelachvili, J. *J. Phys. Chem. B* **1998**, *102*, 234−244.
(9) Green, J.-B. D.; McDermott, M. T.; Porter, M. D. *J. Phys. Chem.* **1996**, *100*, 13342−13345.
(10) Rozsnyai, L. F.; Wrighton, M. S. *Chem. Mater.* **1996**, *8*, 309−311.
(11) Thomas, R. C.; Kim, T.; Crooks, R. M.; Houston, J. E.; Michalske, T. A. *J. Am. Chem. Soc.* **1995**, *117*, 3830−3834.
(12) Laibinis, P. E.; Whitesides, G. M. *J. Am. Chem. Soc.* **1992**, *114*, 9022−9028.
(13) Zamborini, F. P.; Crooks, R. M. *Langmuir* **1998**, *14*, 3279−3286.
(14) Tokuhisa, H.; Zhao, M.; Baker, L. A.; Phan, V. T.; Dermody, D. L.; Garcia, M. E.; Peez, R. F.; Crooks, R. M.; Mayer, T., M. *J. Am. Chem. Soc.* **1998**, *120*, 4492−4501.
(15) Tomalia, D. A.; Naylor, A. M.; Goddard, W. A., III *Angew. Chem., Int. Ed. Engl.* **1990**, *29*, 138−175.
(16) Zeng, F.; Zimmerman, S. C. *Chem. Rev.* **1997**, *97*, 1681−1712.
(17) Schenning, A. P. H. J.; Elissen-Roman, C.; Weener, J.-W.; Baars, M. W. L. P.; van der Gaast, S. J.; Meijer, E. W. *J. Am. Chem. Soc.* **1998**, *120*, 8199−8208.
(18) Wells, M.; Crooks, R. M. *J. Am. Chem. Soc.* **1996**, *118*, 3988−3989.
(19) Zhao, M.; Crooks, R. M. *Angew. Chem., Int. Ed.* **1999**, *38*, 364−366.
(20) Tokuhisa, H.; Crooks, R. M. *Langmuir* **1997**, *13*, 5608−5612.
(21) Zhao, M.; Tokuhisa, H.; Crooks, R. M. *Angew. Chem., Int. Ed. Engl.* **1997**, *36*, 2596−2598.
(22) Hamers, R. J. *J. Phys. Chem.* **1996**, *100*, 13103−13120.
(23) Sauer, B. B.; McLean, R. S.; Thomas, R. R. *Langmuir* **1998**, *14*, 3045−3051.

10.1021/la9903595 CCC: $18.00
Published on Web 08/17/1999

dendrimer monolayers,[25,26] dendrimer multilayers,[27] and dendrimer/*n*-alkylthiol mixed-monolayers[1] have all been recently investigated using AFM.

In our earlier work, dendrimer/*n*-alkylthiol mixed-monolayer films were prepared on two distinctly different types of Au substrates: electron-beam-deposited Au on Ti-primed Si (Si/Ti/Au)[14] and single-crystal Au(111).[1] When either Si/Ti/Au (Au RMS roughness, ~2.0 nm) or single-crystal Au (RMS roughness, ~0.2 nm) were used as substrates, AFM, reflection-infrared spectroscopy, and ellipsometry indicated that exposure of dendrimer monolayers to *n*-alkylthiol solutions for <24 h resulted in coadsorption of the thiol and simultaneous compression of the dendrimers.[1,14] Experiments performed on the flatter Au single crystals indicated that increased *n*-alkylthiol exposure times (~24−48 h) resulted in separation of the dendrimers into distinct domains. At even longer exposure times (>48 h) the *n*-alkylthiols completely displaced the dendrimers from the surface.[1] Dendrimer displacement was not observed on the relatively rough electron-beam deposited substrates even after 10 days. These observations are consistent with previous findings that the tenacity of protein and polymer binding is increased on rough surfaces.[28,29]

Our new findings confirm that mixed dendrimer/*n*-alkylthiol monolayers comprise a dynamic system when formed on extremely smooth Au single-crystal substrates. The nature of phase-segregation and desorption is dependent on dendrimer generation, *n*-alkylthiol chain length, and solvent-dendrimer and substrate-dendrimer interactions. For example, longer *n*-alkyl chains are better able to compete for the sites on the Au surface than are shorter ones, and therefore they induce phase segregation, and ultimately dendrimer desorption, more quickly. We also find that dendrimers only aggregate in the presence of polar solvents, which clearly implicates solvent-dendrimer interactions as a key player in the energetics of this system. Finally, increasing the binding strength of the dendrimers to the surface by modification of the terminal groups with thiols completely inhibits phase separation.

Experimental Section

Chemicals. *n*-Alkylthiols were purchased from the Aldrich Chemical Co. (Milwaukee, WI) and either used as received [$CH_3(CH_2)_4SH$, 95% and $CH_3(CH_2)_{11}SH$, 97%] or vacuum distilled [$CH_3(CH_2)_{15}SH$, 92%]. Amine-terminated Starburst PAMAM dendrimers were obtained from Dendritech, Inc. (Midland, MI) as a 4−20 wt % solution in methanol. The solutions were stored at 4 °C and used as received.

Thiol-terminated dendrimers were synthesized by reacting fourth-generation, amine-terminated PAMAM dendrimers (G4-NH_2) with the *N*-hydroxysuccinimide ester of 3-mercaptopropanoic acid (prepared by reduction of the corresponding disulfide). ^{13}C NMR indicated complete functionalization of the terminal amine groups. Full synthetic details have been reported elsewhere.[30] Monolayers of the thiol-terminated dendrimer (G4-SH) were deposited from a 1 mM solution in $CHCl_3$:EtOH (9:1 by volume).

Preparation of Au(111) Substrates and Mixed-Monolayer Films. Au wire (99.99%; 0.5 mm diameter; Refining Systems Inc.; Las Vegas, NV) was melted and zone-refined in a H_2-rich H_2/O_2 flame. This procedure yields 1.5−2.0 mm diameter beads, which contain atomically smooth, single-crystal (111) facets having terraces up to 1 μm wide.[31−33]

Dendrimer/*n*-alkylthiol mixed-monolayers were prepared by sequential deposition of the dendrimer and then the *n*-alkylthiol. Specifically, the freshly prepared Au(111) substrates were first immersed in an ethanolic solution of the appropriate dendrimer for 18 h. The concentration of the terminal amine groups was kept constant at 6.4×10^{-3} M for the different dendrimer generations, which corresponds to 1.0×10^{-4}, 2.5×10^{-5}, and 6.3×10^{-6} M for G4-NH_2, G6-NH_2, and G8-NH_2, respectively. After rinsing with copious amounts of ethanol, the dendrimer-modified substrates were transferred (while still wet) to a 1.0×10^{-3} M ethanolic solution of the *n*-alkylthiol. Modified substrates were emersed from the *n*-alkylthiol solution after 60 ± 5 s; 60 ± 1 min; 24.0 ± 0.1 h; and 96.0 ± 0.1 h, and again rinsed with ethanol and dried in a flowing stream of dry N_2. Note that different but identically prepared substrates were used for each step in the time-sequenced AFM images presented in the figures. This approach avoids quenching of the morphological evolution of the monolayers, which occurred when the films were allowed to dry. All substrates were prepared at 22 ± 2 °C.

Tapping-Mode Atomic Force Microscopy (TM-AFM). TM-AFM topographical maps of the mixed-monolayer surface were obtained in air using a Digital Instruments Nanoscope III (Santa Barbara, CA) fitted with a 10 μm "e" scanner. Tapping-mode cantilevers (Digital Instruments) had resonance frequencies between 260 and 280 kHz, force constants of 20−100 N/m, and tip apex radii between 5 and 10 nm. Images were acquired with 512×512 pixels at 1.0−2.0 Hz using a near-minimal contacting force.[1,34] The resulting images were flattened and plane-fit using Digital Instruments software. Several images were acquired at random locations on each sample to ensure film uniformity. Bearing analyses, which are used to calculate the fractional surface coverage that lies below a set *z* value, were performed to determine the percentage *n*-alkylthiol coverage in the mixed monolayers. A value just above the top of the *n*-alkylthiol monolayer phase was used as the cutoff.

Results and Discussion

The energetics of the dendrimer/*n*-alkylthiol system can be described in terms of the following individual components: (1) the length of the *n*-alkylthiol chains; (2) the strength and number of Au/dendrimer-functional-group interactions relative to the Au/*n*-alkylthiol energetics; and (3) the relative solvation energy of the dendrimers and *n*-alkylthiols. To gauge the importance of each of these factors, we systematically varied the alkyl chain length, the size of the dendrimers (and thus the number of functional groups in contact with the Au surface), the chemical composition of the dendrimer terminal groups, and the solvent in which the competitive adsorption experiments were performed.

In addition to the two-component dendrimer/*n*-alkylthiol mixed-monolayers, we also analyzed single-component dendrimer monolayers to provide a comparative frame of reference. Figure 1a is a 2×2 μm TM-AFM micrograph of a G4-NH_2 monolayer. The corrugated surface topography differs markedly from the flatter topography observed on single-component *n*-alkylthiol monolayers.[1,27] The roughly circular feature that dominates the image corresponds to a single-atom-deep vacancy island, which is typical of unmodified Au(111). That it is observed here suggests that the dendrimers conformally cover the Au

(24) Tamada, K.; Hara, M.; Sasabe, H.; Knoll, W. *Langmuir* **1997**, *13*, 1558−1566.
(25) Takada, K.; Díaz, D. J.; Abruña, H. D.; Cuadrado, I.; Casado, C.; Alonso, B.; Morán, M.; Losada, J. *J. Am. Chem. Soc.* **1997**, *119*, 10763−10773.
(26) Karthaus, O.; Ijiro, K.; Shimomura, M.; Hellman, J.; Irie, M. *Langmuir* **1996**, *12*, 6714−6716.
(27) Tsukruk, V. V.; Rinderspacher, F.; Bliznyuk, V. N. *Langmuir* **1997**, *13*, 2171−2176.
(28) Lampin, M.; Warocquier-Clérout, R.; Legris, C.; Degrange, M.; Sigot-Luizard, M. F. *J. Biomed. Mater. Res.* **1997**, *36*, 99−108.
(29) Wen, X.; Wang, X.; Zhang, N. *Biomed. Mater. Eng.* **1996**, *6*, 173−189.
(30) Chechik, V.; Crooks, R. M. *Langmuir*, in press.
(31) Zamborini, F. P.; Crooks, R. M. *Langmuir* **1997**, *13*, 122−126.
(32) Ross, C. B.; Sun, L.; Crooks, R. M. *Langmuir* **1993**, *9*, 632−636.
(33) Hsu, T.; Cowley, J. M. *Ultramicroscopy* **1983**, *11*, 239−250.
(34) Bar, G.; Thomann, Y.; Brandsch, R.; Cantow, H.-J.; Whangbo, M.-H. *Langmuir* **1997**, *13*, 3807−3812.

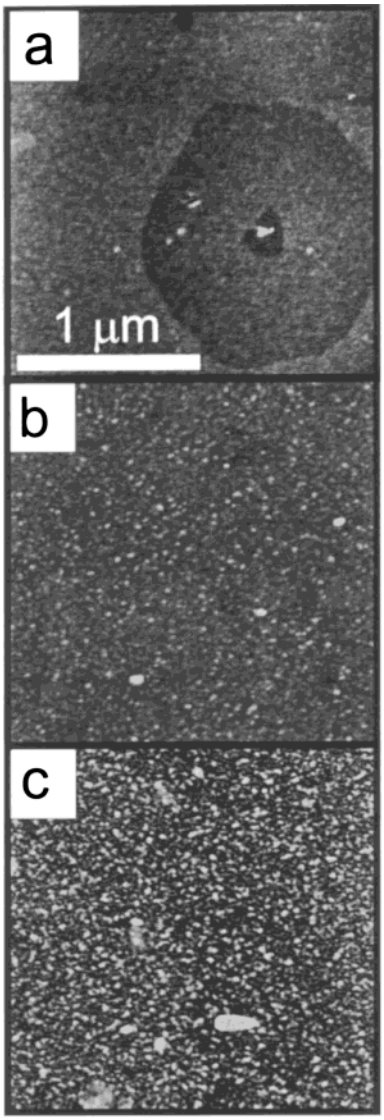

Figure 1. $2 \times 2\ \mu$m TM-AFM topographic images of PAMAM dendrimer monolayers adsorbed to an Au(111) single-crystal surface. (a) G4-NH_2; (b) G6-NH_2; (c) G8-NH_2. The gray scale is 5 nm. The dark circular feature in (a) is a single atom vacancy island present on the Au single crystal.

surface. This island also provides a convenient internal height reference corresponding to the Au(111) step height of 0.235 nm.[35] Parts b and c of Figure 1 show TM-AFM images of G6-NH_2 and G8-NH_2 dendrimer monolayers, respectively. The 2−4 nm high, light-colored features present in these frames result from individual dendrimers. It is not possible to resolve individual G4-NH_2 dendrimers at monolayer coverage because the AFM cantilever apex is large compared to the G4-NH_2 dendrimers (4.5 nm diameter in solution),[15] and because the dendrimer coverage is very high (∼86%).[14] These two factors prevent the AFM tip from accurately sampling the underlying Au between dendrimers. The calculated center-to-center distance between undistorted dendrimers increases for the larger G6-NH_2 (6.7-nm diameter) and G8-NH_2 (9.7-nm diameter),[15] which renders them less susceptible to the just-described imaging problems. Nevertheless, the small interdendrimer spacing for all of the monolayers

(35) The interatomic spacing in Au is reported as 0.28841 nm in *CRC Handbook of Chemistry and Physics*, 68th ed.; Weast, R. C., Ed.; CRC Press: Boca Raton, FL, 1987. The Au(111) step height can be geometrically determined as 0.235 nm.

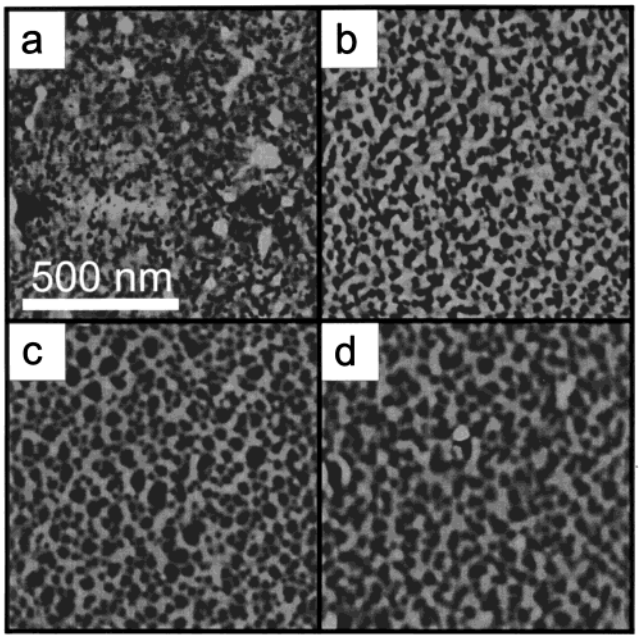

Figure 2. $1 \times 1\ \mu$m TM-AFM topographic images of mixed monolayers prepared by adsorption of G4-NH_2 followed by C5SH. Thiol adsorption times are as follows: (a) 1 min; (b) 1 h; (c) 24 h; (d) 96 h. The gray scale is 10 nm. The black regions present in all 4 images correspond to thiol domains in the mixed-monolayer. The lighter regions correspond to agglomerations of dendrimers.

prevents accurate height measurements. Note, however, that we have previously reported molecularly resolved TM-AFM images of both G4-NH_2 and G8-NH_2, but at much lower surface concentrations.[1]

Figure 2 shows a sequence of four $1 \times 1\ \mu$m TM-AFM micrographs of G4-NH_2 monolayers after exposure to an ethanolic solution of $CH_3(CH_2)_4SH$ (C5SH) for 1 min and 1, 24, and 96 h. The lighter regions, which enlarge as the C5SH exposure time increases, correspond to domains of agglomerated dendrimers. The phase-segregation process begins in less than 1 min (part a of Figure 2), and several domains composed solely of C5SH, which range in size from about 3 to 10 nm, are apparent. These domains are actually slightly larger than they appear because of tip−sample convolution.[36] Part b of Figure 2 shows a micrograph taken after 1 h of C5SH exposure. Inspection of the micrographs reveals that the average size of both the *n*-alkylthiol and dendrimer domains increases with time as the dendrimers agglomerate. Parts c and d of Figure 2 were obtained after 24 and 96 h of *n*-alkylthiol adsorption, respectively, and show an increase in the size of the C5SH domains.

AFM images of the time-dependent adsorption of $CH_3(CH_2)_{11}SH$ (C12SH) to G4-dendrimer-modified surfaces is shown in Figure 3. In comparison to the shorter C5SH, the phase-segregation rate is significantly faster. C12SH is known to form single-component monolayers containing fewer defects than C5SH monolayers,[37,38] and therefore we believe that it exerts a greater lateral force on the dendrimers which helps to drive the agglomeration process. The dendrimer domains in part d of Figure 3 are, on average, larger and higher (10 nm vs 4 nm) than those in part d of Figure 2.

(36) Williams, P. M.; Shakesheff, K. M.; Davies, M. C.; Jackson, D. E.; Roberts, C. J.; Tendler, S. J. B. *Langmuir* **1996**, *12*, 3468−3471.
(37) Porter, M. D.; Bright, T. B.; Allara, D. L.; Chidsey, C. E. D. *J. Am. Chem. Soc.* **1987**, *109*, 3559−3568.
(38) Bain, C. D.; Troughton, E. B.; Tao, Y.-T.; Evall, J.; Whitesides, G. M.; Nuzzo, R. G. *J. Am. Chem. Soc.* **1989**, *111*, 321−335.

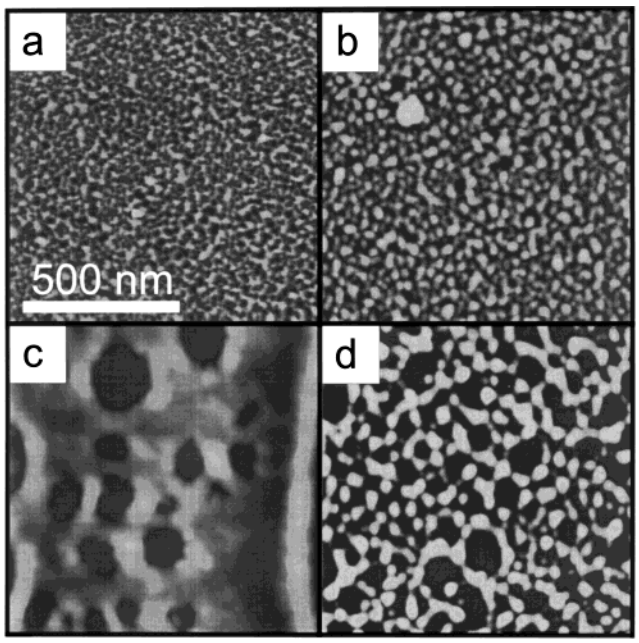

Figure 3. 1 × 1 μm TM-AFM topographic images of mixed monolayers prepared by adsorption of G4-NH_2 followed by C12SH. Thiol adsorption times are as follows: (a) 1 min; (b) 1 h; (c) 24 h; (d) 96 h. The gray scale is 10 nm. The black regions present in all 4 images correspond to thiol domains in the mixed-monolayer. The lighter regions correspond to agglomerations of dendrimers.

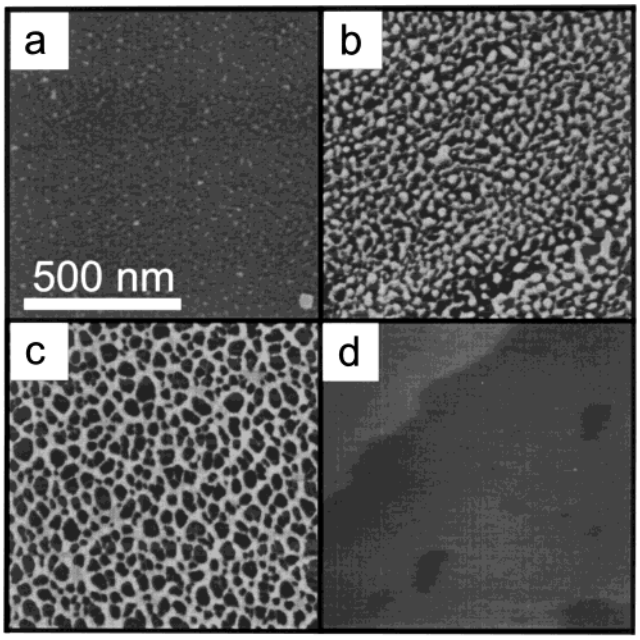

Figure 4. 1 × 1 μm TM-AFM topographic images of mixed monolayers prepared by adsorption of G4-NH_2 followed by C16SH. Thiol adsorption times are are follows: (a) 1 min; (b) 1 h; (c) 24 h; (d) 96 h. The gray scale is 10 nm in (a), (b), and (c). The gray scale in part d is 2 nm. The black regions present in b and c correspond to thiol domains in the mixed-monolayer. In part d the dendrimers have been completely displaced and only C16SH is present on the surface. An Au atomic step is clearly visible in the image.

Figure 4 shows a series of 1 × 1 μm micrographs obtained during exposure of a G4-NH_2 monolayer to $CH_3(CH_2)_{15}$-SH (C16SH). Slight phase segregation is observed after 1 min, but after 24 h (part c of Figure 4) a large network of multilayer dendrimer domains is clearly evident. Remarkably, after 96 h of soaking in the C16SH solution

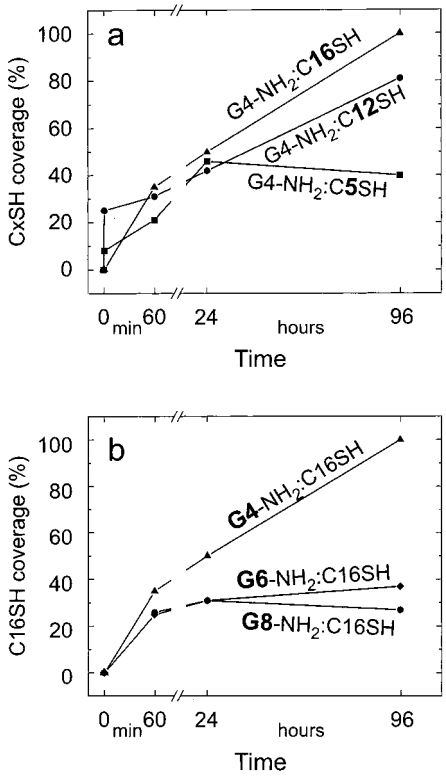

Figure 5. Plots of *n*-alkylthiol surface coverage of dendrimer/*n*-alkylthiol mixed monolayers as a function of thiol soaking time. (a) Three traces which correspond to C5SH, C12SH, and C16SH adsorbed to G4-NH_2 dendrimer monolayers. (b) C16SH adsorbed to G4-NH_2, G6-NH_2, and G8-NH_2 monolayers. The longer *n*-alkylthiols display a greater ability to displace the G4-NH_2 dendrimer monolayer. The larger G6-NH_2 and G8-NH_2 monolayers are less easily displaced by C16SH than G4-NH_2. Percent areas were calculated using the Digital Instruments bearing analysis feature. A height just above the thiol was chosen as a stop-band, all pixels below this stop-band were counted and summed. The data points in each set were obtained 1 min, 1 h, 24 h, and 96 h after immersion of the dendrimer-coated substrates in the *n*-alkylthiol solution.

the dendrimer monolayer is completely displaced from the surface (part d of Figure 4), and the single atomic steps and vacancy islands present on the Au(111) surface are again visible beneath the conformal, 2.1 nm-thick *n*-alkylthiol monolayer.

The data shown in Figures 2−4, which are summarized graphically in part a of Figure 5, indicate that coadsorption of longer *n*-alkylthiols results in faster desorption of the surface-confined G4-NH_2 dendrimers. We believe that dendrimer desorption is roughly correlated to the extent of phase segregation. The relative rates of dendrimer desorption can be rationalized in terms of differences in adsorption energy between the dendrimers and *n*-alkylthiols on the Au surface. In our model, which is represented in Scheme 1, the surface films undergo a series of changes as they progress from dendrimer monolayers to mixed dendrimer/*n*-alkylthiol monolayers, and in some cases to monolayers comprised solely of *n*-alkylthiols. When dendrimer monolayers are exposed to solvated *n*-alkylthiol molecules, the latter bind to the Au substrate at defects and within interstices between dendrimers. This leads to replacement of some Au/amine interactions by stronger Au/thiol bonds.[14] As additional *n*-alkylthiols attach to the surface their alkyl chains align and, due to steric interactions, exert lateral pressure on the dendrimers.[39] The elastic dendrimers then undergo a conformational change from oblate to prolate spheroids, which we have previously

Scheme 1

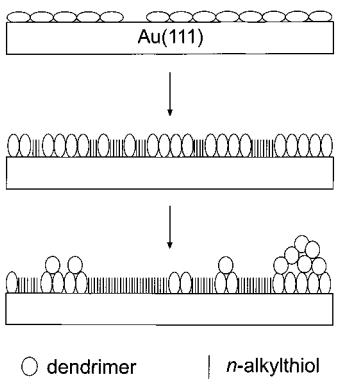

documented.[1,14] As additional *n*-alkylthiols reach the surface, additional Au/amine interactions are lost, which lowers the total dendrimer adsorption energy. These weakly attached dendrimers are able to laterally diffuse short distances on the surface. It is a matter of speculation whether the dendrimers are principally mobile on the Au surface, atop adsorbed *n*-alkylthiol molecules, or both. The latter, however, seems most likely. It is rather unlikely that mass transfer is a consequence of complete dendrimer desorption from the surface followed by readsorption elsewhere, as this would lead to rapid desorption of the entire dendrimer monolayer.

We suggest that aggregation results from mobile dendrimers encountering one another and interacting strongly by, for example, interdigitation or hydrogen bonding.[1] Such interactions are generally not observed in solution.[40] The rate of dendrimer aggregation is kinetically slow due to the large size and mass of the dendrimers (G4-NH_2, 4.5-nm diameter, ~14 500 gm/mol) and the large number of exterior primary amine groups on each dendrimer (G4-NH_2, 64), many of which are in contact with the Au surface. The dendrimer domains eventually ripen into larger 3-D domains up to 25 nm high, which corresponds to about 5 dendrimers. Eventually, the dendrimers furthest from the Au surface, which are the weakest bound, solvate and ultimately desorb from the surface. The extent of this ripening and desorption process depends on the length of the thiol alkyl chains.

To understand the effect of dendrimer size on the agglomeration process, G4-NH_2, G6-NH_2, and G8-NH_2 dendrimer films were exposed to C5SH, C12SH, and C16SH. For example, Figure 6 shows four micrographs resulting from surfaces prepared by coadsorption of C16SH on a G8-NH_2-modified Au substrate for times ranging from 1 min to 96 h. The higher generation dendrimers agglomerate, but at a slower rate than G4-NH_2 (Figure 4). This result is consistent with the larger number of Au/terminal-amine interactions for G8-NH_2 compared to G4-NH_2, which leads to a higher total adsorption energy for G8-NH_2.

Part b of Figure 5 shows the percentage surface coverage of C16SH as a function of time for G4-NH_2, G6-NH_2, and G8-NH_2 monolayers exposed to an ethanolic solution of C16SH. The smaller G4-NH_2 dendrimer completely desorbs from the surface after an exposure time of 96 h, while the domains composed of the higher generation dendrimers still occupy most of the surface area after 96 h. We conclude that the more extensive polypodal interactions experienced by the higher generation dendrimers lead to monolayers that desorb and phase separate more slowly than the lower generation materials.

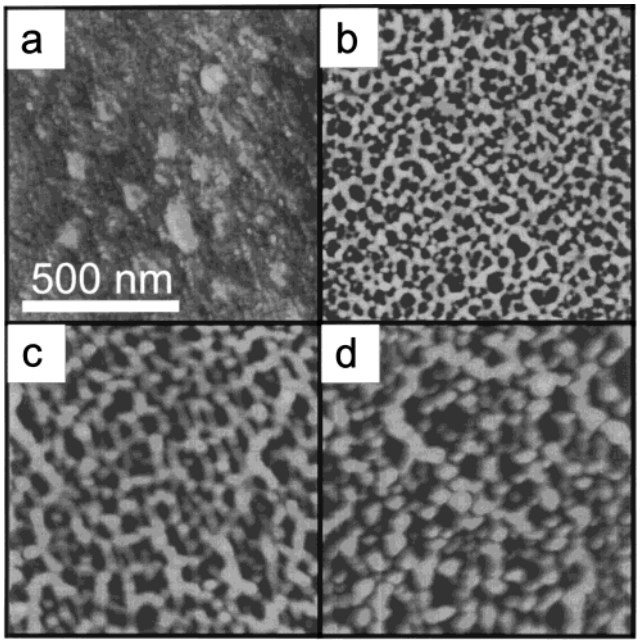

Figure 6. $1 \times 1\ \mu$m TM-AFM topographic images of a G8-NH_2 monolayer following exposure to C16SH for: (a) 1 min; (b) 1 h; (c) 24 h; (d) 96 h. The gray scale is 10 nm. The lighter regions correspond to agglomerations of dendrimers, and the darker regions correspond to C16SH regions.

In an effort to better understand the role played by the dendrimer endgroups during *n*-alkylthiol-driven phase separation and desorption, we prepared monolayers composed of fourth-generation dendrimers having thiol terminal groups (G4-SH). By analogy to *n*-alkylthiols, the dendrimers terminated in thiols should adhere better to the Au surface than the amine-terminated dendrimers, and we predicted that the monopodal *n*-alkylthiols would not be able to compete for Au surface sites with the polypodal dendrimers.[41] Part a of Figure 7 shows a TM-AFM image of a single-component G4-SH monolayer. Part b shows an identically prepared monolayer after immersion in the ethanolic C16SH solution for 96 h. It is evident that neither phase separation nor agglomeration of the dendrimers occurs.

On the basis of the data in Figure 7, we conclude that the magnitude of the dendrimer-terminal-group interaction energy is a primary factor in determining the extent of phase-segregation in dendrimer/*n*-alkylthiol mixed-monolayers. However, the solvent in which competition between dendrimer and *n*-alkylthiol takes place is also important. That is, apparently the *n*-alkylthiols are unable to bind to the surface unless dendrimer primary amine groups desorb. If this supposition is correct, then phase segregation should be slowed or eliminated when the *n*-alkylthiols are coadsorbed to a dendrimer-modified surface from a poor solvent for the dendrimer terminal groups.[14] To test this hypothesis, we performed *n*-alkylthiol coadsorption from *n*-hexane. Part c of Figure 7 shows a micrograph of a single-component G4-NH_2 monolayer, and part d shows such a monolayer after exposure to an *n*-hexane solution of C16SH for 24 h. There are significant differences in the two images, probably because of C16SH adsorption at interstices between dendrimers, but there

(39) Berger, R.; Delamarche, E.; Lang, H. P.; Gerber, C.; Gimzewski, J. K.; Meyer, E.; Güntherodt, H.-J. *Science* **1997**, *276*, 2021−2024.

(40) Uppuluri, S.; Tomalia, D. A.; Dvornic, P. R. *Proceedings of the ACS Division Polymeric Materials*; American Chemical Society: Washington, DC, 1997; Vol. 77, pp 116−117.

(41) Xu, C.; Sun, L.; Kepley, L. J.; Crooks, R. M.; Ricco, A. J. *Anal. Chem.* **1993**, *65*, 2102−2107.

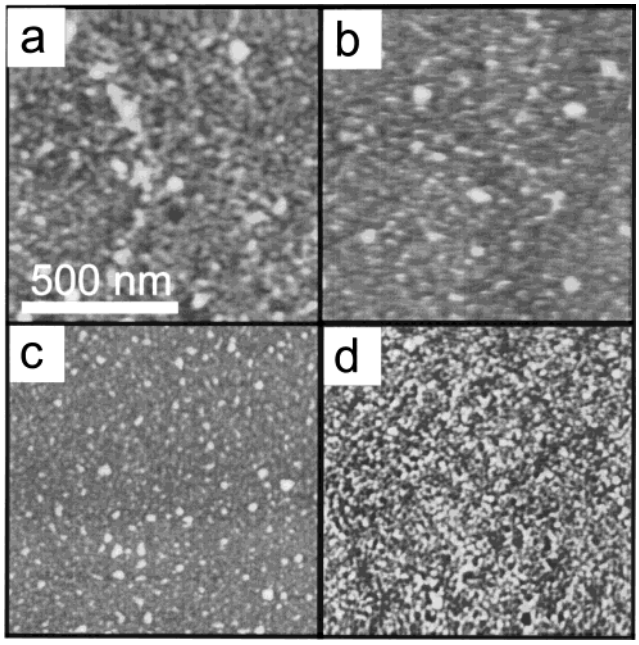

Figure 7. 1 × 1 μm TM-AFM topographic images showing the effect of changing the terminal group and solvent on dendrimer mobility. (a) Single-component G4-SH monolayer; (b) G4-SH/C16SH mixed monolayer after 96 h exposure to the thiol. There is no discernible dendrimer agglomeration after 96 h exposure to the C16SH. (c) 1 × 1 μm TM-AFM images of G4-NH_2; (d) 1 × 1 μm TM-AFM image obtained after exposure of a G4-SH monolayer to C16SH dissolved in hexane for 24 h. There is no discernible agglomeration after 24 h. The gray scale is 10 nm.

is no evidence for extensive phase segregation (compare with part c of Figure 4).

Dendrimer domain sizes measured in this study typically have diameters ranging from 5 to 50 nm. Such domains are well represented in the high-resolution micrographs discussed thus far. However, the G4-NH_2 dendrimer monolayers occasionally exhibit phase segregation on a much larger length scale. Part a of Figure 8 shows a 10 × 10 μm TM-AFM micrograph of a G4-NH_2 monolayer after exposure to C12SH for 24 h. Two distinct regions are visible in the image. The lower-right part of the figure contains C12SH-only domains on which Au atomic features are clearly visible through the SAM. The weblike structure at the upper left is a large dendrimer/C12SH mixed-monolayer domain. The 1 × 1 μm box near the center of the figure is the region of this surface presented in part c of Figure 3. Part b of Figure 8 shows a TM-AFM scan along the line in part a. At the boundary between the C12SH domain and the mixed G4-NH_2/C12SH domain, the dendrimers are present as multilayers rising more than 25 nm (corresponding to at least 5 dendrimer diameters) above the C12SH monolayer. Within the mixed domain, the dendrimer regions are lower: ~8 nm above the C12SH monolayer. Results similar to those shown in Figure 8 were also observed for one of the G4-NH_2 monolayers after extended exposure to an ethanolic solution of C16SH. We think that these infrequently observed structures result from a late stage in the dendrimer desorption process. At this late stage, interdendrimer aggregation occurs, but the resulting metastable structures are likely not in contact with much, if any, of the Au surface and thus readily desorb.

Summary and Conclusions

We have described a dynamic phase-segregation process involving dendrimer/*n*-alkylthiol mixed-monolayers con-

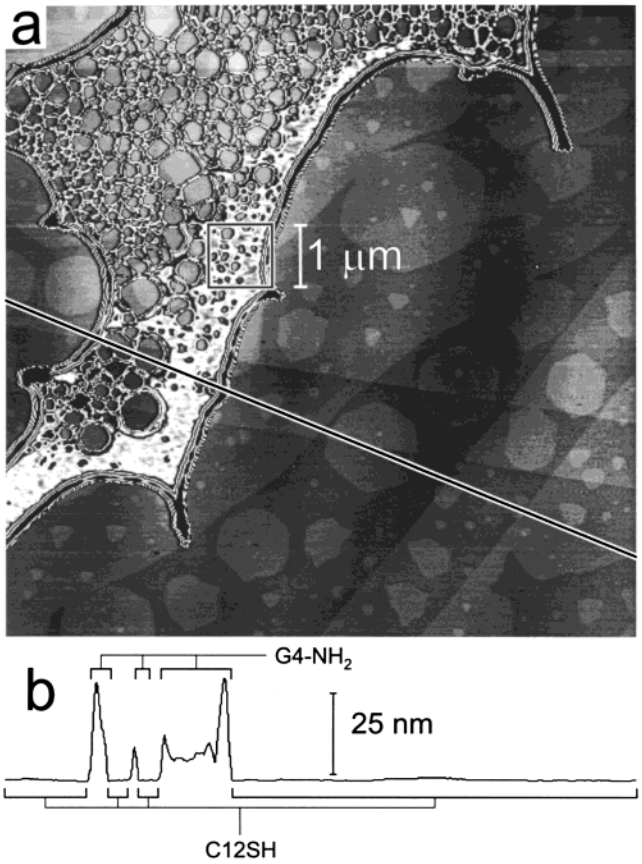

Figure 8. (a) A 10 × 10 μm TM-AFM topographic image of a G4-NH_2 monolayer after exposure to C12SH for 24 h. The large weblike structure in the upper left is a domain of agglomerated dendrimers. Au atomic steps and vacancy islands are visible under the thiol domain regions. The square near the center of the image indicates the region of this image presented in part c of Figure 3. (b) A line-scan displaying the heights of the dendrimer domains in relation to the thiol monolayer.

fined to Au(111) surfaces. TM-AFM micrographs of dendrimer-only monolayers reveal homogeneous surfaces in which individual high-generation dendrimers can be molecularly resolved. When monolayers of amine-terminated dendrimers confined to these smooth Au substrates are immersed in ethanolic solutions of *n*-alkylthiols, the latter compete for the surface and cause the dendrimers to distort, phase-segregate, and ultimately to desorb (Scheme 1). This process begins within 1 min of exposure to *n*-alkylthiols of any length. For the smallest dendrimers (G4-NH_2), adsorption of the longest *n*-alkylthiol (C16SH) causes the greatest amount of phase change; in fact, the G4-NH_2 dendrimer is completely displaced from the Au surface after exposure to C16SH for 96 h (part d of Figure 4).

We propose a model that accounts for these findings in which the longer *n*-alkylthiols compete more successfully with the dendrimers for Au surface sites, and in which smaller dendrimers are more weakly bound to the Au surface (and are thus more susceptible to displacement) than those of higher generation. Indeed, the G6-NH_2 and G8-NH_2 PAMAM dendrimers undergo significantly slower phase segregation and desorption than G4-NH_2, because the former have a greater number of Au/terminal-amine interactions per dendrimer. Dendrimer motion on the surface is driven by the presence of the *n*-alkylthiol coadsorbate. That is, in a good solvent (such as ethanol) for the amine-terminated dendrimers, the interaction between the Au surface and a single amine group is rather

weak even though the aggregate of these interactions for a single dendrimer is significant. Thus, the *n*-alkylthiols can compete with individual amines for adsorption locations on the Au substrate. Displacement of an amine group by a thiol renders the Au/dendrimer interaction weaker. When enough amine groups are displaced the dendrimer becomes mobile and phase segregation ensues. Because the dendrimer domains are closely spaced and generally interconnected, we suspect that the dendrimers do not diffuse too far from their original locations on the surface. Relatively strong interdendrimer interactions lead to dendrimer aggregation, including multilayer formation. However, these aggregates solubilize and eventually desorb.

Functionalization of the G4 terminal groups with thiol groups prevents phase segregation and desorption, which clearly indicates that a very strong interaction between the dendrimers and Au renders the dendrimers immobile. Phase segregation and desorption slow considerably when *n*-alkylthiol exposure takes place in a poor solvent for the dendrimer terminal groups. This finding was illustrated by coadsorbing the *n*-alkylthiol from hexane.

We conclude that the two-dimensional phase dynamics of this system are driven by a delicate balance between the Au/dendrimer interaction energy (which is dominated by the dendrimer terminal groups), the total adsorption energy of the *n*-alkylthiols (which is a function of the chain length), and the solvation energy of the dendrimer terminal groups. Moreover, the presence of multilayer dendrimer structures suggests that interdendrimer interactions, such as interdigitation and hydrogen bonding, also figure prominently in the description of this interesting system. We have also shown that phase separation occurs on two length scales, although we have only discussed the smaller of these in detail in this study.

Acknowledgment. We gratefully acknowledge the National Science Foundation (CHE-9818302) and the Robert A. Welch Foundation for support of this work. We also thank Mr. Mark Kaiser (Dendritech, Inc., Midland, MI) for helpful discussions, providing technical information, and for supplying the amine-terminated Starburst PAMAM dendrimers used in this study. We also thank Dr. Andreas Hierlemann (ETH, Zürich) for helpful discussions.

LA9903595